



HHS Public Access

Author manuscript

Nat Commun. Author manuscript; available in PMC 2013 October 09.

Published in final edited form as:

Nat Commun. 2013 ; 4: 1662. doi:10.1038/ncomms2677.

FBXW7 α attenuates inflammatory signalling by downregulating C/EBP δ and its target gene *Tlr4*

Kuppusamy Balamurugan¹, Shikha Sharan¹, Kimberly D. Klarmann², Youhong Zhang¹, Vincenzo Coppola³, Glenn H. Summers⁴, Thierry Roger⁵, Deborah K. Morrison¹, Jonathan R. Keller², and Esta Sterneck^{1,*}

¹Laboratory of Cell and Developmental Signaling, National Cancer Institute-Frederick, P.O. Box B., Frederick, MD 21702-1201 ²Basic Science Program, SAIC-Frederick, Inc., Laboratory of Cancer Prevention, National Laboratory for Cancer Research, P.O. Box B., Frederick, MD 21702-1201 ³Department of MVIMG, Wexner Medical Center, Ohio State University-Comprehensive Cancer Center, Ohio State University-CCC, 988 Biological Research Tower 460 West 12th Avenue, Columbus, OHIO 43210 ⁴Laboratory Animal Sciences Program, SAIC-Frederick, NCI, FNLCR, Frederick, MD ⁵Infectious Diseases Service, Centre Hospitalier Universitaire Vaudois and University of Lausanne, BH 19-111, rue du Bugnon 46, CH-1011 Lausanne, Switzerland

Abstract

Toll-like receptor 4 (TLR4) plays a pivotal role in innate immune responses, and the transcription factor CCAAT/enhancer binding protein delta (C/EBP δ , *Cebpd*) is a TLR4-induced gene. Here, we identify a positive feedback loop in which C/EBP δ activates *Tlr4* gene expression in macrophages and tumour cells. In addition, we discovered a negative feedback loop whereby the tumour suppressor FBXW7 α (FBW7, Cdc4), whose gene expression is inhibited by C/EBP δ , targets C/EBP δ for degradation when C/EBP δ is phosphorylated by GSK-3 β . Consequently, FBXW7 α suppresses *Tlr4* expression and responses to the ligand lipopolysaccharide (LPS). FBXW7 α depletion alone is sufficient to augment pro-inflammatory signalling *in vivo*. Moreover, as inflammatory pathways are known to modulate tumour biology, *Cebpd* null mammary tumours, which have reduced metastatic potential, show altered expression of inflammation-associated genes. Together, these findings reveal a role for C/EBP δ upstream of TLR4 signalling and uncover a function for FBXW7 α as an attenuator of inflammatory signalling.

Innate immune responses to infection are induced in part by Toll-like receptors (TLRs), which belong to the pattern recognition receptor family. To date, 10 human and 12 mouse TLRs are known, each of which binds specific ligands. TLR4 recognises lipopolysaccharide (LPS) from Gram-negative bacteria and signals in combination with other co-receptors to

Users may view, print, copy, download and text and data- mine the content in such documents, for the purposes of academic research, subject always to the full Conditions of use: http://www.nature.com/authors/editorial_policies/license.html#terms

*Correspondence: sterneck@mail.nih.gov.

Competing interests:

The authors declare no competing financial interests.

activate the NF- κ B transcription factors¹. TLR4 is involved in diseases such as sepsis and chronic inflammatory disorders^{2,3}. TLR4 signalling in tumour cells is associated with suppression of immune surveillance, proliferation, inflammatory cytokine production, and invasive migration⁴⁻⁸. Therefore, understanding the regulation of TLR4 expression and signalling may be important for the management of these conditions.

C/EBP δ is an inflammatory response gene⁹. C/EBP δ amplifies LPS signalling, and it is essential for the expression of many LPS-induced genes and the clearance of Gram-negative bacterial infection¹⁰. *Cebpd* deficiency partly protects mice from LPS-induced mortality and autoimmune encephalomyelitis, suggesting that C/EBPTM has a role in the progression of systemic inflammatory diseases such as sepsis and multiple sclerosis^{11,12}.

We reported that C/EBP δ directly inhibits the expression of the F-box and WD repeat domain containing protein 7 alpha (FBXW7 α) in mammary tumour cells¹³. The *Fbxw7* gene encodes three protein isoforms, of which the alpha isoform is the most abundantly expressed¹⁴. FBXW7 functions as the substrate-recognition subunit of SCF-type ubiquitin ligase complexes. FBXW7 α targets various mammalian oncoproteins for degradation, including c-myc, cyclin E, mTOR, c-jun and Notch^{14,15}. We also showed that hypoxia-induced C/EBP δ inhibited the expression of FBXW7 α , resulting in elevated levels of mTOR and consequently hypoxia-inducible factor 1 alpha (HIF-1 α)¹³. HIF-1 α is a subunit of the HIF-1 transcription factor complex and is necessary for cellular adaptation to hypoxia. HIF-1 target genes promote angiogenesis and the metabolic switch to glycolysis, which augments survival under hypoxia¹⁶. In agreement with the role of hypoxia and HIF-1 α in tumour metastasis^{17,18}, loss of *Cebpd* results in reduced metastatic progression of MMTV-Neu-induced mammary tumours¹³. MMTV-Neu transgenic mice express the rat tyrosine kinase receptor Neu (ERBB2/HER2) specifically in mammary epithelial cells, mimicking the overexpression of ERBB2 observed in 30% of human breast cancers¹⁹. Although *Cebpd*-deficient MMTV-Neu-transgenic mice are 50% less likely than wild-type mice to develop metastases, these mice also exhibit a 50% increased tumour multiplicity compared to controls¹³; these observations are in agreement with other tumour-suppressor like activities of C/EBP δ , such as suppression of cyclin D1 expression^{13,20,21}.

HIF-1 α also promotes macrophage activation and inflammatory responses, as does the FBXW7 α target Notch^{22,23}. However, the role of FBXW7 α in inflammatory signalling has not been addressed. Because C/EBP δ augments HIF-1 α expression in tumour cells¹³, and both C/EBP δ and HIF-1 α are known to mediate inflammatory responses, we hypothesised that the C/EBP δ -FBXW7-HIF-1 pathway played a role in macrophage activation. Here, we show that C/EBP δ augments HIF-1 α expression and pro-inflammatory signalling in activated macrophages through the inhibition of FBXW7 α expression. We also found that C/EBP δ acts upstream of LPS signalling by directly activating *Tlr4* gene expression. In addition, we identified a negative feedback loop where FBXW7 α downregulates C/EBP δ that is phosphorylated by GSK-3 β . These results identify a novel role for FBXW7 α as a suppressor of inflammatory gene expression.

RESULTS

LPS and C/EBP δ inhibit FBXW7 α expression in macrophages

We previously reported that C/EBP δ directly inhibits *Fbxw7a* gene expression in tumour cells, which in turn augments HIF-1 α expression¹³. To investigate this pathway in macrophages, we first analysed FBXW7 isoform expression. Semi-quantitative analysis suggested that macrophages and mammary tumours expressed only *Fbxw7a* mRNA but not *Fbxw7b* or *Fbxw7c*, while all three isoforms were detected in mouse embryo fibroblasts (Fig. 1a). In mouse primary peritoneal macrophages (PPMs), basal levels of *Fbxw7a* mRNA were higher in *Cebpd*^{-/-} (KO) compared to wild-type (WT) macrophages. LPS treatment decreased *Fbxw7a* transcripts in WT but not in KO macrophages (Fig. 1b). The silencing of *CEBPD* by RNAi in U-937 human monocytic cells increased the basal level of *FBXW7* mRNA and abolished its repression upon LPS treatment (Supplementary Fig. S1a). Next, we analysed resident peritoneal exudate cells (PECs), which consisted of approximately 67 \pm 2.7% macrophages/monocytes, 23 \pm 1% lymphoid cells, and 4.9 \pm 0.6% neutrophils independent of genotype (mean \pm S.E.M, n=4 mice). *In vivo* LPS treatment (6 h) reduced FBXW7 α protein levels in WT PECs but not in *Cebpd*^{-/-} cells, while C/EBP δ expression was induced by this treatment in WT PECs (Supplementary Fig. S1b). Furthermore, the higher levels of basal FBXW7 α that were observed in *Cebpd*^{-/-} PECs (Supplementary Fig. S1b, c) were correlated with reduced levels of its targets mTOR and Aurora A and reduced phosphorylation of AKT, S6K1 and GSK-3 β (Supplementary Fig. S1c). Taken together, these data show that macrophages express FBXW7 α and that FBXW7 α expression is downregulated by C/EBP δ and LPS.

C/EBP δ and FBXW7 α control HIF-1 α expression in monocytes

LPS and hypoxia cooperatively induce HIF-1 α expression in macrophages²⁴, and we confirmed these results in ANA-1 mouse macrophages (Supplementary Fig. S1d). Under these conditions, primary human monocytes treated with *CEBPD* RNAi had increased FBXW7 α expression and reduced HIF-1 α accumulation (Fig. 1c). As expected¹³, *CEBPD* depletion also increased *FBXW7a* mRNA levels (Fig. 1d). Interestingly, FBXW7 α depletion increased the levels of C/EBP δ and HIF-1 α protein (Fig. 1c) and of *CEBPD* mRNA (Fig. 1d), demonstrating that FBXW7 α suppresses C/EBP δ expression. In *Cebpd*^{-/-} PPMs, HIF-1 α accumulation could be rescued by knockdown of the elevated FBXW7 α (Fig. 1e). These results demonstrate that C/EBP δ promotes HIF-1 α expression in activated macrophages through the inhibition of FBXW7 α expression, as previously reported for mammary tumour cells¹³.

HIF-1 is critical for hypoxia-induced glycolysis in macrophages²². Therefore, we examined if reduced HIF-1 α expression in *Cebpd* null PECs affected their glycolytic activity and activation. Under inflammatory conditions (LPS+1% O₂), *Cebpd* null PECs exhibited reduced hallmarks of the glycolytic switch, such as glucose consumption and lactate generation (Supplementary Fig. S1e). In agreement with these data, ATP production and the survival of *Cebpd* null peritoneal cells were reduced under these conditions (Supplementary Fig. S1f–g). Furthermore, *Cebpd*-deficient peritoneal macrophages exhibited limited induction of pro-inflammatory genes, such as *Mmp9*, *Cxcr4*, *Vegfc* and *Il6*, after stimulation

with LPS+1% O₂ (Supplementary Fig. S1h). These genes are known HIF-1 targets¹⁸, *Il6* and *Cxcr4* are also direct targets of C/EBP δ ^{10,13}. Collectively, these findings show that C/EBP δ supports HIF-1-mediated inflammatory responses.

Importantly, there was no difference in the number of PECs isolated from *Cebpd*^{-/-} mice compared with the controls. However, there was a small but significant decrease in the number of PPMs isolated from *Cebpd*^{-/-} mice after elicitation, and there was a significant decrease in the recruitment of peritoneal cells upon LPS treatment *in vivo* (Supplementary Fig. S2a, b). An analysis of baseline myeloid haematopoiesis suggests that myeloid development is normal in *Cebpd*^{-/-} mice (see Supplementary Note 1 and Fig. S2c–j). Thus, we conclude that the functional differences detected in the macrophages from *Cebpd*^{-/-} mice are not due to developmental defects.

FBXW7 α targets C/EBP δ for degradation

FBXW7 α is not a transcription factor. Therefore, its downregulation of *Cebpd* mRNA levels must be through indirect mechanisms. Because C/EBP δ can activate its own promoter¹⁰ and has a degron-like sequence commonly found in FBXW7 substrates^{14,15}, we investigated whether FBXW7 α regulated C/EBP δ expression at the protein level. Pulse-chase analysis (Fig. 2a) and cycloheximide-chase experiments (Supplementary Fig. S3a) showed that the half-life of C/EBP δ protein increased significantly when *Fbxw7a* was silenced in RAW 264.7 macrophages. Furthermore, inhibition of the proteasome by MG132 increased the basal expression of C/EBP δ and revealed its polyubiquitination, which was significantly reduced upon *Fbxw7a* silencing (Fig. 2b and Supplementary Fig. S3b). In *Fbxw7a*-silenced cells, MG132 did not further increase C/EBP δ protein levels. In contrast, ectopic FBXW7 α ²⁵ further decreased the half-life of C/EBP δ and increased its polyubiquitination (Supplementary Fig. S3c, d). Co-immunoprecipitation assays showed that ectopic and endogenous C/EBP δ physically interacted with FBXW7 α (Supplementary Fig. S3e). These results indicate that FBXW7 α is required for the ubiquitination and degradation of C/EBP δ in RAW 264.7 macrophages. Accordingly, C/EBP δ binding to its own promoter increased when *Fbxw7a* was silenced (Supplementary Fig. S3f). Collectively, these data demonstrate a negative feedback loop from FBXW7 α to C/EBP δ .

FBXW7-substrate interaction requires a phospho-degron motif, which is also present in C/EBP δ (Fig. 2c). To investigate the role of this motif, we mutated the potential phospho-acceptor residues serine and threonine to alanine (TTS/AAA). Figure 2d shows that FBXW7 α decreased the steady-state levels of the ectopic wild-type C/EBP δ but not the TTS/AAA mutant. Co-immunoprecipitation assays revealed that the degron motif of C/EBP δ was necessary for its interaction with FBXW7 α (Fig. 2e). Indeed, FBXW7 α mediated the polyubiquitination of WT- but not TTS/AAA-C/EBP δ *in vitro* (Fig. 2f), and the degron motif was required for polyubiquitination *in vivo* (Fig. 2g). Next, we generated a TTS/DDD mutation to mimic its phosphorylation, and we confirmed that this protein interacted with FBXW7 α (Fig. 2h). The half-life of TTS/DDD-C/EBP δ was significantly reduced compared to the stabilisation observed with the TTS/AAA mutation (Fig. 2i). In the presence of MG132, WT- and TTS/DDD-C/EBP δ were expressed at similar steady-state levels; these findings corroborated the notion that the low levels of TTS/DDD-C/EBP δ were due to

degradation (Fig. 2j). Collectively, these data show that degnon-phosphorylation regulates the stability of C/EBP δ .

GSK-3 β regulates C/EBP δ protein stability

The serine/threonine kinase GSK-3 β is responsible for the phosphorylation of most FBXW7 α substrates¹⁴. Indeed, phospho-threonine could be detected on WT-C/EBP δ expressed in RAW 264.7 cells, but this phosphorylation was significantly reduced by the GSK-3 β inhibitor CHIR or the TTS/AAA mutation (Fig. 3a). Consistent with this result, the GSK-3 β inhibitors CHIR or BIO increased the expression of C/EBP δ in PPMs and RAW 264.7 cells (Fig. 3b). In contrast, the expression of TTS/DDD-C/EBP δ was not increased by CHIR (Fig. 3c). These results suggest a role for the GSK-3 β pathway in the regulation of C/EBP δ expression. Indeed, *in vitro* kinase assays with recombinant activated GSK-3 β confirmed that GSK-3 β directly phosphorylated C/EBP δ (Fig. 3d). The TTS/AAA mutation significantly reduced C/EBP δ phosphorylation, and phospho-peptide analysis confirmed that GSK-3 β targets T156 of the degnon (Fig. 3d and Table 1). Phosphorylation at S160 was also detected but to a much lesser extent. In addition, T49 was phosphorylated by GSK-3 β *in vitro* on both WT- and TTS/AAA-C/EBP δ . This residue is not conserved across species and its role, if any, remains to be determined.

Our results show that GSK-3 β phosphorylation attenuates C/EBP δ levels in untreated macrophages. Next, we investigated the role of this pathway in activated macrophages. LPS signalling inhibits GSK-3 β through the PI3K/AKT pathway²⁶. LPS reduced threonine-phosphorylation of C/EBP δ , which was consistent with an increase in the inhibitory Ser9-phosphorylation on GSK-3 β (Fig. 3e) and in the half-life of C/EBP δ (Fig. 3f). Furthermore, ectopic active GSK-3 β -S9A²⁷ (Fig. 3g) or pharmacological inhibition of PI3K/AKT reduced LPS-induced C/EBP δ expression (Fig. 3h). These data show that LPS activates C/EBP δ expression at least in part by inhibition of the GSK-3 β /FBXW7 α pathway.

FBXW7 α regulates TLR4 expression through C/EBP δ

Because FBXW7 α targeted C/EBP δ for degradation, FBXW7 α could have a role in attenuating pro-inflammatory signalling. To test this hypothesis, we expressed FBXW7 α ²⁵ in PPMs to mimic the elevated levels of FBXW7 α in *Cebpd* null cells (Supplementary Fig. S4a). FBXW7 α suppressed all tested responses of PPMs to LPS, such as the expression of iNOS, C/EBP δ , p65, Notch-intracellular-domain (NICD) and COX-2 and the phosphorylation of ERK1/2 and STAT3 (Fig. 4a). Similar data were obtained with RAW 264.7 macrophages (Supplementary Fig. S4b). Furthermore, the transcript levels of *Nos2*, *Cebpd*, *Il6*, *Vegfc*, and *Mmp9* were significantly reduced by ectopic FBXW7 α in PPMs (Fig. 4b), as was NO production and the glycolytic switch in response to LPS+1% O₂ (Supplementary Fig. S4c, d). These data are reminiscent of the phenotype of *Cebpd* null cells, which express elevated levels of FBXW7 α . The profound suppression of LPS-responses by ectopic FBXW7 α suggested that upstream elements in the LPS signalling pathway were downregulated by FBXW7 α . Intracellular LPS signalling is initiated by TLR4¹. Indeed, ectopic FBXW7 α reduced expression of TLR4 along with C/EBP δ in PPMs (Fig. 4c), while RNAi against *Fbxw7a* increased the basal and LPS-induced levels of TLR4 and C/EBP δ (Fig. 4d). In addition, several pro-inflammatory markers, such as NICD, iNOS

and p65, were induced by *Fbxw7a*-silencing alone (Fig. 4d). These data prompted the hypothesis that FBXW7 α regulates TLR4 expression through C/EBP δ . The depletion of C/EBP δ prevented the upregulation of TLR4 in response to *Fbxw7a* silencing (Fig. 4e), demonstrating that C/EBP δ mediates TLR4 upregulation. Even basal expression of TLR4 depended on C/EBP δ . Lastly, co-expression of degradation-resistant TTS/AAA-C/EBP δ with FBXW7 α rescued TLR4 expression in RAW 264.7 macrophages, demonstrating that FBXW7 α downregulates TLR4 through the inhibition of C/EBP δ expression (Fig. 4f).

FBXW7 α suppresses inflammatory signaling

Increased basal levels of TLR4 and C/EBP δ protein due to RNAi against *Fbxw7a* were also observed in RAW 264.7 macrophages, along with increased transcript levels of the pro-inflammatory genes *Cebpd*, *Tlr4*, *Tnfa*, *Il6*, *Nos2* and *Mmp9* in PPMs (Supplementary Fig. S5a, b). Taking this approach further, we silenced *Fbxw7a* *in vivo* by intraperitoneal injection of siRNA. *In vivo* RNAi can cause non-specific effects that include activation of the immune system²⁸. Indeed, control siRNAs led to a modest increase of C/EBP δ expression in PECs compared to vehicle treatment (Supplementary Fig. S5c). In comparison, two *Fbxw7a* RNAi oligos caused a greater increase in both C/EBP δ and TLR4 protein levels. Following this pilot experiment, *Ctrl1* and *Fbxw7a1* siRNA were used for subsequent analyses. Peritoneal cells that were isolated two days after the injection of *Fbxw7a* siRNA exhibited reduced FBXW7 α levels and higher basal expression of C/EBP δ , TLR4, NICD, p65, and iNOS protein compared with control siRNA (Fig. 4g). In addition, transcripts for *Cebpd*, *Nos2* and *Il6* were induced (Supplementary Fig. S5d). More cells were recovered from *Fbxw7a*-siRNA treated mice, indicating the activation of recruitment pathways (Supplementary Fig. S5e). However, the ratios of different PECs was not altered (Supplementary Fig. S5f). Furthermore, *Fbxw7a* siRNA resulted in detectable levels of plasma IL-6 in otherwise untreated mice and in increased IL-6 concentrations in LPS-treated mice (Fig. 4h). These data show that endogenous FBXW7 α is necessary to prevent pro-inflammatory gene expression. RNAi depletion of FBXW7 α in PPMs sensitised the cells, such that 1 ng/ml LPS elicited a response that was comparable to 10–100 ng in control cells, as measured by the expression of C/EBP δ and p65 and the phosphorylation of ERK and p38 MAP kinase (Fig. 4i). Note that *Fbxw7* RNAi increased the basal TLR4 protein levels to LPS-induced levels at this 4 h time point. Taken together, these data show that FBXW7 α attenuates the LPS response through inhibition of C/EBP δ and TLR4 expression and that FBXW7 α -depletion alone is sufficient to activate inflammatory signalling.

TLR4 is a direct transcriptional target of C/EBP δ

Because C/EBP δ promoted TLR4 protein expression, we next addressed the mechanism underlying this regulation. The loss of C/EBP δ in KO PECs or RNAi-depleted RAW 264.7 macrophages reduced *Tlr4* mRNA levels (Fig. 5a). Similarly, overexpression of FBXW7 α suppressed *Tlr4* mRNA levels (Fig. 5b), which was consistent with the induced *Tlr4* mRNA levels upon *Fbxw7a* silencing (Supplementary Fig. S5b). Interestingly, the expression of *Tlr2*, *Tlr4*, and *Tlrs 5–9* was also reduced in *Cebpd*-deficient PPMs, while the expression of *Tlr1* and *Tlr3* was increased (Supplementary Fig. S5g). These data implicate C/EBP δ in the regulation of most *Tlr* genes. Because of our aforementioned data, we focused our subsequent analyses on TLR4. Inspection of the *Tlr4* promoter sequence revealed putative

C/EBP binding sites within 200 bp upstream of the transcription start site (Fig. 5c). ChIP analysis of PPMs demonstrated the binding of C/EBP δ to the proximal *Tlr4* promoter region but not to a distal promoter region, where there were no putative binding sites (Fig. 5c). Consistent with these data, *Cebpd* RNAi or FBXW7 α overexpression both reduced the activity of a *Tlr4* promoter-luciferase reporter construct (Fig. 5d). Next, we assessed the effect of TLR4 reconstitution in *Cebpd* null PPMs (Fig. 5e). Overexpression of TLR4²⁹ in WT PPMs had no significant effect on the LPS-induced expression of *Nos2* and *Il6*. In *Cebpd*-deficient macrophages, however, ectopic TLR4 significantly enhanced LPS-induction of *Nos2* and *Il6* transcripts (Fig. 5f). C/EBP δ binds the *Il6* promoter¹⁰ and may regulate the *iNOS* promoter directly³⁰. Our data show that the impaired LPS response of *Il6* and *Nos2* in *Cebpd* null macrophages is in part due to reduced TLR4 levels, and it is less due to the role of C/EBP δ as a downstream effector of TLR4. The role of basal C/EBP δ expression was further supported by an analysis of early LPS signalling events. The accumulation of p65 and the phosphorylation of ERK, p38 and JNK kinases in response to LPS were attenuated in *Cebpd* null PPMs within 30–60 min of treatment (Fig. 5g). In summary, these results show that C/EBP δ also functions upstream of LPS signalling through activation of *Tlr4* gene expression.

C/EBP δ augments inflammatory signalling in tumours

TLR4 is expressed in both macrophages and tumour cells⁴. Proteins such as HMGB1 and S100A8 act as ligands that activate TLR4 signalling, and these ligands are important in tissue repair, inflammatory diseases, and cancer^{3,31,32}. Inflammation-associated gene expression is strongly correlated with tumour malignancy³³. Given that C/EBP δ promotes metastatic progression of MMTV-Neu mammary tumours¹³, we investigated whether C/EBP δ modulates TLR4 expression in tumour cells. Stable depletion of C/EBP δ in a mouse mammary tumour cell line or in human MCF-7 breast tumour cells reduced TLR4 protein expression and induced FBXW7 α levels (Fig. 6a). Analyses of MMTV-Neu tumour tissue confirmed the reduced *Tlr4* mRNA, increased *Fbxw7* mRNA, and, on average, lower TLR4 protein levels in *Cebpd*^{-/-} tumours compared with WT (Fig. 6b). In addition, iNOS protein expression (Fig. 6b) and *Il6*, *Nos2*, *Arg1*, and *Tnfa* transcript levels were lower in *Cebpd*^{-/-} tumours (Fig. 6c). Interestingly, the transcript levels of *Il10* and *Il13*, which are expressed in cells including alternatively activated macrophages and T cells, were significantly higher in *Cebpd*^{-/-} tumours (Fig. 6c). The inverse correlation of *Cebpd* and *Il10* expression *in vivo* is consistent with a previous report on C/EBP δ functions in dendritic cells¹².

We also examined the expression of chemokines and chemokine receptors, which play an important role in breast tumour progression and metastasis³⁴. *Cebpd* KO tumours exhibited significantly reduced expression of the metastasis-promoting gene *Cxcr4*, which was consistent with our previous report that C/EBP δ directly regulates *Cxcr4* in cultured mammary tumour cells⁵. In contrast, C/EBP δ -null tumours exhibited increased expression of *Ccl3* and *Ccl5*, which augment T-cell mediated anti-immune responses³⁵ (Supplementary Fig. S6). Of these genes, the *Ccl3* gene promoter is directly activated by C/EBP δ after LPS induction⁴. Collectively, these data show that the loss of C/EBP δ leads to complex alterations of pro- and anti-inflammatory genes in mammary tumour tissue and that this

complexity may be due to its multifaceted roles in macrophages and mammary epithelial cells.

Macrophages and tumour cells engage in crosstalk, and a metastasis-promoting paracrine loop has been described with breast carcinoma cells producing colony stimulating growth factor-1 (CSF-1) and macrophages expressing epidermal growth factor (EGF)³⁶. We found that both *Csf1* and *Egf* expressions were significantly reduced in *Cebpd* null MMTV-Neu mammary tumours (Fig. 6d). Though further analyses will be required to dissect the contribution of different cell types to these observations, the results are likely due to C/EBP δ action in both the immune cells and tumour cells. In summary, these data show that C/EBP δ activity profoundly affects the expression of proteins that are modulators of the immune system, which collectively creates a largely pro-inflammatory microenvironment in mammary tumours.

DISCUSSION

In this study, we identified a positive feedback loop between C/EBP δ and TLR4 and a negative feedback loop between C/EBP δ and FBXW7 α , which together modulate TLR4 signalling and pro-inflammatory gene expression (Fig. 7). Phosphorylation of C/EBP δ by GSK-3 β is required for its degradation by FBXW7 α . Therefore, inhibition of GSK-3 β by LPS stabilises C/EBP δ . Identification of TLR4 as a direct transcriptional target of C/EBP δ renders C/EBP δ a pro-inflammatory factor upstream of TLR4 in addition to its functions downstream.

Macrophages can be activated by several pathways, and C/EBP δ together with C/EBP β also participates in Fc γ receptor-mediated inflammatory cytokine and chemokine production and in IgG IC-stimulation of macrophages³⁷. In addition to our data, the regulation of *Tlr8* expression by C/EBP δ as well as its binding to the *Tlr6* gene promoter have been reported^{10,38}. A critical role of C/EBP δ in LPS responses has previously been shown *in vitro* and *in vivo*. *Cebpd* null mice are hypersensitive to persistent bacterial infection¹⁰ and hyposensitive to septic shock after sensitisation¹¹. Both phenotypes were attributed to the role of C/EBP δ as an inflammatory response gene and regulator of target genes such as *Il6*. Furthermore, the role of C/EBP δ in amplifying LPS signalling has been described³⁹. It should be noted that one study reported that C/EBP δ is dispensable for LPS-induced *Il6* expression⁴⁰. It remains to be determined which experimental details are responsible for the difference in results.

Our findings place C/EBP δ upstream of LPS signalling for expression of the TLR4 receptor. The loss of C/EBP δ does not abolish *Tlr4* expression entirely, which explains why LPS responses are not completely impaired. Interestingly, our data from reconstituting *Cebpd*^{-/-} cells with ectopic TLR4 suggest that the precise role of C/EBP δ downstream of TLR signalling should be re-evaluated in light of its role in regulating TLR4 expression. Low dose LPS specifically induces C/EBP δ expression rather than NF-kB⁴¹, supporting the notion that C/EBP δ is critical in sensitising cells to LPS.

Our data show that C/EBP δ promotes macrophage activation in part by augmenting HIF-1 α expression. Inflamed tissue is hypoxic and HIF-1 mediates hypoxia adaptation by regulating the transcription of many genes associated with angiogenesis, glycolysis, and migration¹⁶. C/EBP δ also promotes tumour lymphangiogenesis through HIF-1⁴². Our results show that macrophage functions that require HIF-1 are blunted in the absence of C/EBP δ because of *Fbxw7a* derepression. HIF-1 α expression in the myeloid lineage also promotes the differentiation of myeloid-derived tumour suppressor cells (MDSCs), which contribute to tumour progression^{17,18,43}. This mechanism may underlie the pro-metastatic function of C/EBP δ in addition to the role of this pathway in epithelial-derived tumour cells¹³.

Interestingly, TLR4 is also a target of HIF-1⁴⁴; hence, C/EBP δ induces TLR4 expression directly under normoxia and also indirectly through HIF-1 induction under hypoxia. This effect provides an additional positive feedback loop because C/EBP δ is a hypoxia-induced gene that is likely downstream of HIF-1^{13,42}. However, this pro-inflammatory loop requires simultaneous inhibition of FBXW7 α expression by C/EBP δ , suggesting that FBXW7 α serves as an important brake on inflammatory signalling.

In this study, we found that *Cebpd*-deficient mouse mammary tumour tissues, which exhibit reduced metastatic progression¹³, express increased FBXW7 α and reduced TLR4 levels. The effects of TLR4 signalling on cancer appear complex and may depend not only on the cell type but also on the stage of tumour development^{6,7,45–48}. In our study, reduced TLR4 expression in *Cebpd* null tumours correlated with mostly reduced pro-inflammatory and increased anti-inflammatory gene expression. This result may be due to the role of C/EBP δ in mammary tumour cells and infiltrating immune cells, direct targeting by C/EBP δ , or indirect downstream effects. Interestingly, reduced innate immune responses in *Cebpd* null mice are also consistent with the increased mammary tumour multiplicity in these mice¹³. Our data warrant further dissection of the role of C/EBP δ in tumour-associated macrophages and their crosstalk with mammary tumour cells, which will be addressed by conditional gene deletion in future analyses.

From this study, FBXW7 α emerged as a potent attenuator of inflammatory signalling. This activity is at least in part due to suppression of C/EBP δ expression at the protein and mRNA levels and is likely to affect not only *Cebpd* but also other genes/proteins that modulate inflammation. Therefore, our data lay the groundwork for further analyses of FBXW7 α functions in the modulation of immune cells. We also suggest that the tumour suppressor activity of FBXW7¹⁴ could be in part due to its role as an attenuator of pro-inflammatory gene expression. According to the “1000 Genomes” catalogue (www.1000genomes.org), the *FBXW7* gene harbours several SNPs, some with possibly deleterious effects on function. We suggest that these SNPs be included in genome-wide association studies of inflammatory diseases. Given the role of FBXW7 α as a suppressor of inflammatory signalling (as shown in this study) and as a *bona fide* tumour suppressor^{14,15}, FBXW7 α is an unlikely therapeutic target. However, better knowledge of the regulation of its expression and its target proteins may provide new avenues for the management of inflammation-associated diseases.

METHODS

Reagents and antibodies

Lipopolysaccharide (LPS from *E. coli*; L4524) was purchased from Sigma-Aldrich, St. Louis, MO. CHIR99021 and BIO (6-Bromoindirubin-3'-oxime) were obtained from Stemgent, San Diego, CA. Antibodies were obtained from the following sources: Cell Signaling Technology (pGSK-3 β -Ser9, #9336; pAKT-Ser473, #4060; pS6K1-Thr389, #9205; pSTAT3, #9145; AKT, #4691; GSK-3 β , #9315; S6K1, #9202; STAT3, #4904; Cleaved Notch-1, #2421S; phospho-p44/42 MAPK-Thr202/Tyr204 (pErk1/2), #9101; p44/42 MAPK (Erk1/2), #9102; pp38-Thr180/Tyr182, #9215S; p38, #9212; pSAPK/JNK-Thr183/Tyr185, #4668S; SAPK/JNK, #9258; phospho-threonine, #9386S); Abcam (iNOS, #ab-15323; F4/F80, #ab-60343-100; Cox-2, #ab-15191; p65 (RelA), #ab-16502; FBXW7, ab#12292); BD Pharmingen (CD11b (M1/70), #550993; GR1, #553128; CD16/CD32, #553142); Novus Biologicals (HIF-1 α , #NB100-449; HIF-1 β , #NB-100-124); Santa Cruz (actin, sc-1616; Ubiquitin, sc-8017); Calbiochem (mTOR, #OP97); Orbigen (FBXW7 α , #PAB-10563); BD Biosciences (Aurora A, #610938); Imgenex (TLR4, #IMG-578A); Bethyl Laboratories (H2AX, #A300-083A); eBioscience (B220, #RA3-6B2; CD3e, #500A-2, and isotype controls); Roche (HA, #11867423001; clone3F10); and Rockland (Tubulin, #600-401-880). The mouse monoclonal antibody clone L46-743.92.69 (batch BD69319) against C/EBP δ was provided by BD Biosciences Pharmingen as an outcome of an Antibody Co-development Collaboration with the NCI.

For information on plasmids see Supplementary Methods.

Mice and isolation of peritoneal cells

Cebpd wild-type and knockout mice⁴⁹ were of the FVB/N strain background (except for data in Supplementary Fig. S2, which are from 129S1 mice) and derived from heterozygous mates. The MMTV-c-Neu tumour model has been described^{13,19}. The subjects were littermates whenever possible. NCI-Frederick (FNLCR) is accredited by AAALLC International and follows the Public Health Service Policy for the care and use of laboratory animals. All experiments were conducted according to protocols approved by the Institutional Animal Care and Use Committee.

For the isolation of PPMs, mice were injected with 3% Brewer thioglycollate medium⁵⁰ in the peritoneal cavity. Four days later, mice were euthanised, and 10 ml sterile PBS (Ca²⁺/Mg²⁺-free) was injected into the peritoneal cavity. The resulting peritoneal fluid was collected and centrifuged at 400 \times g for 10 min at 4°C. The cell pellet was washed once with PBS. Erythrocytes were lysed with sterile water, and the final pellet was suspended in 1:1 DMEM/F12 medium with 10% foetal bovine serum (FBS). Viability was >95%. Cell preparations were characterised by FACS analysis using antibodies that distinguish macrophages from other hematopoietic cells. On average, 82.5 \pm 3.7% (mean \pm S.E.M., n=6) of the cells were Mac-1⁺ and F4/80⁺ before plating. The isolated cells were plated and allowed to adhere for 2 h. Non-adherent cells were washed off with PBS, and new culture medium was added. Cells were cultured for 24 h before experimental treatments.

Resident peritoneal exudate cells (PECs) were isolated as described above but without prior elicitation by thioglycollate. For details, see Supplementary Methods.

Cell culture

MMTV-Neu and MCF-7 cell lines with stable depletion of C/EBP δ were generated by transfection of expression constructs for shRNA against C/EBP δ (or GFP as a control¹³). Cells were selected in G418 and maintained as pools. ANA-1, RAW 264.7 mouse macrophages and HEK293T cells were cultured in DMEM containing 10% FBS. PPMs and PECs were cultured in DMEM/F12 medium containing 10% FBS. The U-937 human monocytic cell line and elutriated primary human monocytes were cultured in RPMI medium containing 5% FBS. The MMTV-Neu mouse mammary tumour cell line (a kind gift of Dr. William Muller, McGill University) was cultured in DMEM containing 5% FBS and 1X-MEGS (mammary epithelial cell growth supplement). Unless indicated otherwise, LPS was used at 100 ng/ml for 16–24 h.

Peripheral blood-derived monocytes were isolated from healthy donors by counterflow centrifugal elutriation under protocols approved by the Institutional Review Boards of both the National Institute of Allergy and Infectious Diseases and the Department of Transfusion Medicine of the National Institutes of Health after appropriate informed consent.

Transient transfections and RNAi

Cells were transfected by nucleofection using the Amaxa Cell-line Nucleofector Kit V (Cat# VCA-1003; Lonza AG). A GFP expression construct was included in all transfections to monitor transfection efficiency. The total amount of DNA in each transfection was kept constant by complementation with vector control DNA. All control samples were transfected with vector only. At 24 h post-transfection, cells were treated as indicated. *Cebpd* siRNA oligos were purchased from Dharmacon (#L-003210-00). *Fbxw7*-specific siRNAs (Silencer predesigned) with the following sequences were used^{13,51}. *Fbxw7a* RNAi-1: 5'-GGGCAGCAGCGGCGGAGGAdTdT-3' and antisense: 5'-UCCUCCGCCGUCGUGCCCCdTdT-3'. *Fbxw7a* RNAi-2: Sense: 5'-GCACAGAAUUGAUACAACCTT-3' and antisense: 5'-GUUAGUAUCAAUUCUGUGCTG-3'. *Fbxw7a* RNAi-3: 5'-GUGAAGUUGUUGGAGUAGAdTdT-3' and antisense: 5'-UCUACUCCAACAACUUCACdTdT-3'. *Fbxw7* RNAi-4: Sense: 5'-GCACAGAAUUGAUACAACCTT-3' and antisense: 5'-GUUAGUAUCAAUUCUGUGCTG-3'. For silencing *Fbxw7a* in mouse cells, *Fbxw7a* RNAi-1 (*in vitro* and *in vivo*) and RNAi-2 (*in vivo*) were used. *Fbxw7a* RNAi-3 and *Fbxw7* RNAi-4 were used at a 1:1 ratio in human cells.

Scrambled siRNA (#D-001960-01-05, Dharmacon) or EGFP siRNA⁵¹ (5'-CAAGCTGACCCTGAAGTTC-3') were used as controls.

For *in vivo* RNAi, mice were injected in the peritoneum with *in vivo*-jetPEITM (Polyplus) according to the manufacturer's instructions. For details see Supplementary Methods.

Western Analysis and In vitro ubiquitination assay

See Supplementary Methods

Pulse-Chase Experiment

RAW264.7 cells were transfected with control or *Fbxw7a* siRNA oligonucleotides. Two days later, the cells were pre-incubated for 30 min in DMEM without methionine and cysteine, pulsed with Tran³⁵S-label (ICN; 300 μ Ci/ml; 1 μ Ci = 37 kBq) for 20 min, and chased with DMEM/10% FBS plus 20 mM methionine and cysteine for the indicated times. Cells were lysed under denaturing conditions, and proteins were immunoprecipitated with anti-CEBPTM antibody and protein G beads. After SDS-PAGE, the dried gel was processed for phosphorimaging. Signals were quantified by ImageQuant software and plotted using GraphPad Prism 5.

Plasma IL-6 measurement

FVB/N mice were injected intraperitoneally with control or *Fbxw7a* siRNA (100 μ g) using *in vivo*-jetPEITM (Polyplus) according to the manufacturer's instructions. Three days later, mice were injected with LPS (40 ng) or vehicle (saline) and euthanised 1 h later to collect heparinised blood. IL-6 was measured in plasma using a mouse IL-6 single analyte ELISA kit according to the manufacturer's instructions (SA Biosciences, Qiagen, USA, # SEM03015A).

RNA isolation and quantitative real-time PCR

RNA was isolated using TRIZOL (Invitrogen), and cDNA was synthesised with Superscript reverse transcriptase III (RT) according to the manufacturer's instructions (Invitrogen, CA). PCR was performed with Taqman gene expression primer/probe sets using the 7500 Fast Real Time PCR instrument (Applied Biosystems). Analysis was performed using the MxPro Software (Stratagene). All reactions were performed in duplicates with "no RT" as the control, and all data are mean \pm S.E.M. of at least three independent biological replicates. The relative expression levels were measured using the relative quantitation (RQ) Ct method and normalised to β -actin. The probe sets (Applied Biosystems) were as follows:

Cebpd: Mm00786711_s1; *Fbxw7a*: Mm01209394_m1; *Tlr4*: Mm00445273_m1; *Il6*: Mm59999064_m1; *Mmp9*: Mm00442991_m1; *Cxcr4*: Mm01292123_m1; *Vegfc*: Mm01202432; *Nos2*: Mm00440502; *Tnfa*: Mm00443258_m1; *Il10*: Mm00439614_m1; *Arg1*: Mm00475988_m1; *Il13*: Mm00434204_m1; *mCsf-1*: Mm00432686_m1; *Egf*: Mm01316968_m1; *Ccl3*: Mm00441259_g1; *Ccl5*: Mm01302427_m1; *Actin*: 4352933-0711018.

Chromatin Immunoprecipitation (ChIP) assay

ChIP analysis was performed per the manufacturer's instructions (EZ ChIP, #17-371 RF, Millipore, USA). PPMs at 80–90% confluency were cross-linked, and the chromatin was prepared and sonicated to an average size of 500 bp. The DNA fragments were immunoprecipitated with antibodies specific to C/EBP δ (5 μ g; BD69319) or control mouse IgG at 4°C overnight. RAW 264.7 macrophages were nucleofected with control or *Fbxw7* siRNA oligos. Forty-eight hours later, cells were processed as above. After reversal of the

cross-linking, the immunoprecipitated chromatin was amplified by PCR as follows: *Tlr4*, 1 cycle of 94°C 3 min, 35 cycles of 94°C 20 sec, 56°C 30 sec, and 72°C 30 sec, and 1 cycle of 72°C 2 min; *Zbrk1*, 1 cycle of 94°C 3 min, 37 cycles of 94°C 20 sec, 56°C 30 sec and 72°C 30 sec, and 1 cycle of 72°C 2 min. *Cebpd*, 1 cycle of 94°C 3 min, 40 cycles of 94°C 20 sec, 56°C 30 sec, and 72°C 30 sec, and 1 cycle of 72°C 2 min. The primers were as follows:

Tlr4 proximal: *Tlr4*-(S): 5'-ACAAGACACGGCAACTGATG-3'

Tlr4-(AS): 5'-GCTTTCATCCCAGGAAGTCA-3'

Tlr4 distal: *Tlr4*-(S): 5'-GCCAAGAAGCTCCACAGAG-3'

Tlr4-(AS): 5'-CATCACTAGTCCAGTCGATACCC-3'

Cebpd: *Cebpd*-(S): 5'-TGATCCCTGTTCCGCCTTTGCTAT-3'

Cebpd-(AS): 5'-AGTGGGTCCGAGACCGGA-3'

Zbrk1: *Zbrk1*-(S): 5'-CATTCTCTGGGATACCTACACCTG -3'

Zbrk1(AS): 5'-CTGTAAAATGGCCGCGCCCATAGC -3'

***In vitro* kinase assay**

For *in vitro* phosphorylation analysis, C/EBP δ was immunoprecipitated with anti-C/EBP δ antibody from radioimmunoprecipitation assay (RIPA) buffer extracts of HEK293T cells transfected with WT or TTS/AAA C/EBP δ and incubated with 100 ng recombinant GSK-3 β in kinase assay buffer, as described previously⁵². Samples were resolved on SDS-PAGE gels and subjected to autoradiography. The labelled C/EBP δ proteins were digested from the gel with pepsin and analysed by reverse-phase high-performance liquid chromatography (HPLC), phosphoamino acid analysis (PAA) and Edman degradation⁵².

Luciferase reporter assay

RAW 264.7 cells were transfected with TLR4 promoter luciferase reporter constructs⁵³, renilla luciferase expression plasmids along with the indicated expression constructs. To silence C/EBP δ expression, two different short hairpin RNA expression constructs were used at 1:1 ratio, and shRNA against green fluorescent protein (GFP) was used as control¹³. Forty-eight hours later, luciferase activity was assessed using a luciferase assay kit according to manufacturer's instructions (Promega).

Metabolic Measurements

Measurements of lactate, glucose, ATP and NO were as described in Supplementary Methods.

Statistical analysis

Unless stated otherwise, quantitative data were analysed by the two-tailed unequal variance t-test and are shown as the mean \pm S.E.M. The number of samples (n) refers to biological replicates.

Supplementary Material

Refer to Web version on PubMed Central for supplementary material.

ACKNOWLEDGEMENTS

This research was supported by the Intramural Research Program of the NIH, Frederick National Lab, National Cancer Institute and in part with Federal Funds from the Frederick National Laboratory (NIH) under contract no. HHSN261200800001E. We are thankful to the SAIC Laboratory Animal Sciences Program for excellent support and to the Department of Transfusion Medicine, Clinical Center, NIH, for providing elutriated monocytes. We thank Suzanne Specht and Linda Miller for excellent technical support, Kathleen Noer for technical assistance with flow cytometry, and Jennifer Mariano for her support with the metabolic labeling studies. For generously providing reagents, we thank Allan Weissman, Ira Daar, Alan Perantoni, William J. Muller (MMTV-Neu tumour cells), Keiichi I. Nakayama, Jian-Hua Mao and Johan Ericsson (Fbxw7 expression plasmids). We thank Giorgio Trinchieri, Howard Young, Peter Johnson and Andrew Hurwitz for helpful discussion and critical comments on the manuscript, Robert Leighty for help with the statistical analysis, Allan Weissman, Yien Che Tsai, Jennifer Mariano, Yoo-Seak Hwang, Arman Bashirova, Min Zhou and C. Andrew Stewart for valuable advice, and Jiro Wada and Allen Kane for preparation of the figures. The content of this publication does not necessarily reflect the views of policies of the Department of Health and Human Services, nor does mention of trade names, commercial products, or organisations imply endorsement by the U.S. Government.

REFERENCES

1. Kawai T, Akira S. Toll-like receptors and their crosstalk with other innate receptors in infection and immunity. *Immunity*. 2011; 34:637–650. [PubMed: 21616434]
2. Roger T, et al. Protection from lethal gram-negative bacterial sepsis by targeting Toll-like receptor 4. *Proc Natl Acad Sci U S A*. 2009; 106:2348–2352. [PubMed: 19181857]
3. Lin Q, Li M, Fang D, Fang J, Su SB. The essential roles of Toll-like receptor signaling pathways in sterile inflammatory diseases. *Int Immunopharmacol*. 2011; 11:1422–1432. [PubMed: 21600309]
4. Huang B, et al. Toll-like receptors on tumor cells facilitate evasion of immune surveillance. *Cancer Res*. 2005; 65:5009–5014. [PubMed: 15958541]
5. Szczepanski MJ, et al. Triggering of Toll-like receptor 4 expressed on human head and neck squamous cell carcinoma promotes tumor development and protects the tumor from immune attack. *Cancer Res*. 2009; 69:3105–3113. [PubMed: 19318560]
6. Liao SJ, et al. Triggering of Toll-like receptor 4 on metastatic breast cancer cells promotes alphavbeta3-mediated adhesion and invasive migration. *Breast Cancer Res Treat*. 2012; 133:853–863. [PubMed: 22042369]
7. Yang H, et al. Reduced expression of Toll-like receptor 4 inhibits human breast cancer cells proliferation and inflammatory cytokines secretion. *J Exp Clin Cancer Res*. 2010; 29:92. [PubMed: 20618976]
8. Zhao Y, et al. Metadherin mediates lipopolysaccharide-induced migration and invasion of breast cancer cells. *PLoS One*. 2011; 6:e29363. [PubMed: 22195048]
9. Ramji DP, Foka P. CCAAT/enhancer-binding proteins: structure, function and regulation. *Biochem J*. 2002; 365:561–575. [PubMed: 12006103]
10. Litvak V, et al. Function of C/EBPdelta in a regulatory circuit that discriminates between transient and persistent TLR4-induced signals. *Nat Immunol*. 2009; 10:437–443. [PubMed: 19270711]
11. Slofstra SH, et al. Gene expression profiling identifies C/EBPdelta as a candidate regulator of endotoxin-induced disseminated intravascular coagulation. *Am J Respir Crit Care Med*. 2007; 176:602–609. [PubMed: 17600275]
12. Tsai VWW, et al. Ccaat/enhancer binding protein-delta expression by dendritic cells regulates CNS autoinflammatory disease. *J Neuroscience*. 2011; 31:17612–17621. [PubMed: 22131422]
13. Balamurugan K, et al. The tumour suppressor C/EBPdelta inhibits FBXW7 expression and promotes mammary tumour metastasis. *EMBO J*. 2010; 29:4106–4117. [PubMed: 21076392]
14. Welcker M, Clurman BE. FBW7 ubiquitin ligase: a tumour suppressor at the crossroads of cell division, growth and differentiation. *Nat Rev Cancer*. 2008; 8:83–93. [PubMed: 18094723]

15. Cheng Y, Li G. Role of the ubiquitin ligase Fbw7 in cancer progression. *Cancer Metastasis Rev.* 2012; 31:75–87. [PubMed: 22124735]
16. Semenza GL. HIF-1: upstream and downstream of cancer metabolism. *Curr Opin Genet Dev.* 2010; 20:51–56. [PubMed: 19942427]
17. Wong CC, et al. Hypoxia-inducible factor 1 is a master regulator of breast cancer metastatic niche formation. *Proc Natl Acad Sci U S A.* 2011; 108:16369–16374. [PubMed: 21911388]
18. Lu X, Kang Y. Hypoxia and hypoxia-inducible factors: master regulators of metastasis. *Clin Cancer Res.* 2010; 16:5928–5935. [PubMed: 20962028]
19. Guy CT, et al. Expression of the neu protooncogene in the mammary epithelium of transgenic mice induces metastatic disease. *Proc Natl Acad Sci U S A.* 1992; 89:10578–10582. [PubMed: 1359541]
20. Pawar SA, et al. C/EBPdelta targets cyclin D1 for proteasome-mediated degradation via induction of CDC27/APC3 expression. *Proc Natl Acad Sci U S A.* 2010; 107:9210–9215. [PubMed: 20439707]
21. Sarkar TR, et al. Identification of a Src tyrosine kinase/SIAH2 E3 ubiquitin ligase pathway that regulates C/EBPdelta expression and contributes to transformation of breast tumor cells. *Mol Cell Biol.* 2012; 32:320–332. [PubMed: 22037769]
22. Cramer T, et al. HIF-1alpha is essential for myeloid cell-mediated inflammation. *Cell.* 2003; 112:645–657. [PubMed: 12628185]
23. Outtz HH, Wu JK, Wang X, Kitajewski J. Notch1 deficiency results in decreased inflammation during wound healing and regulates vascular endothelial growth factor receptor-1 and inflammatory cytokine expression in macrophages. *J Immunol.* 2010; 185:4363–4373. [PubMed: 20739676]
24. Frede S, Stockmann C, Freitag P, Fandrey J. Bacterial lipopolysaccharide induces HIF-1 activation in human monocytes via p44/42 MAPK and NF-kappaB. *Biochem J.* 2006; 396:517–527. [PubMed: 16533170]
25. Mao JH, et al. FBXW7 targets mTOR for degradation and cooperates with PTEN in tumor suppression. *Science.* 2008; 321:1499–1502. [PubMed: 18787170]
26. Martin M, Rehani K, Jope RS, Michalek SM. Toll-like receptor-mediated cytokine production is differentially regulated by glycogen synthase kinase 3. *Nat Immunol.* 2005; 6:777–784. [PubMed: 16007092]
27. Wang H, et al. IFN-beta production by TLR4-stimulated innate immune cells is negatively regulated by GSK3-beta. *J Immunol.* 2008; 181:6797–6802. [PubMed: 18981097]
28. Marques JT, Williams BR. Activation of the mammalian immune system by siRNAs. *Nat Biotechnol.* 2005; 23:1399–1405. [PubMed: 16273073]
29. Roger T, David J, Glauser MP, Calandra T. MIF regulates innate immune responses through modulation of Toll-like receptor 4. *Nature.* 2001; 414:920–924. [PubMed: 11780066]
30. Won JS, Im YB, Key L, Singh I, Singh AK. The involvement of glucose metabolism in the regulation of inducible nitric oxide synthase gene expression in glial cells: possible role of glucose-6-phosphate dehydrogenase and CCAAT/enhancing binding protein. *J Neuroscience.* 2003; 23:7470–7478. [PubMed: 12930785]
31. Zhang Z, Schluesener HJ. Mammalian toll-like receptors: from endogenous ligands to tissue regeneration. *Cellular and molecular life sciences : CMLS.* 2006; 63:2901–2907. [PubMed: 17072502]
32. Hiratsuka S, et al. The S100A8-serum amyloid A3-TLR4 paracrine cascade establishes a pre-metastatic phase. *Nat Cell Biol.* 2008; 10:1349–1355. [PubMed: 18820689]
33. Grivennikov SI, Greten FR, Karin M. Immunity, inflammation, and cancer. *Cell.* 2010; 140:883–899. [PubMed: 20303878]
34. Karnoub AE, Weinberg RA. Chemokine networks and breast cancer metastasis. *Breast Dis.* 2006; 26:75–85. [PubMed: 17473367]
35. Gonzalez-Martin A, Gomez L, Lustgarten J, Mira E, Manes S. Maximal T cell-mediated antitumor responses rely upon CCR5 expression in both CD4(+) and CD8(+) T cells. *Cancer Res.* 2011; 71:5455–5466. [PubMed: 21715565]

36. Goswami S, et al. Macrophages promote the invasion of breast carcinoma cells via a colony-stimulating factor-1/epidermal growth factor paracrine loop. *Cancer Res.* 2005; 65:5278–5283. [PubMed: 15958574]
37. Yan C, Zhu M, Staiger J, Johnson PF, Gao H. C5a-regulated CCAAT/enhancer binding protein beta and -delta are essential in Fc gamma receptor-mediated inflammatory cytokine and chemokine production in macrophages. *J Biol Chem.* 2012; 287:3217–3230. [PubMed: 22147692]
38. Zannetti C, et al. C/EBP{delta} and STAT-1 are required for TLR8 transcriptional activity. *J Biol Chem.* 2010; 285:34773–34780. [PubMed: 20829351]
39. Kravchenko VV, Mathison JC, Schwamborn K, Mercurio F, Ulevitch RJ. IKKi/IKKepsilon plays a key role in integrating signals induced by pro-inflammatory stimuli. *J Biol Chem.* 2003; 278:26612–26619. [PubMed: 12736252]
40. Lu YC, et al. Differential role for c-Rel and C/EBPbeta/delta in TLR-mediated induction of proinflammatory cytokines. *J Immunol.* 2009; 182:7212–7221. [PubMed: 19454718]
41. Maitra U, Gan L, Chang S, Li L. Low-Dose Endotoxin Induces Inflammation by Selectively Removing Nuclear Receptors and Activating CCAAT/Enhancer-Binding Protein {delta}. *J Immunol.* 2011; 186:4467–4473. [PubMed: 21357541]
42. Min Y, et al. C/EBP-delta regulates VEGF-C autocrine signaling in lymphangiogenesis and metastasis of lung cancer through HIF-1alpha. *Oncogene.* 2011; 30:4901–4909. [PubMed: 21666710]
43. Corzo CA, et al. HIF-1alpha regulates function and differentiation of myeloid-derived suppressor cells in the tumor microenvironment. *J Exp Med.* 2010; 207:2439–2453. [PubMed: 20876310]
44. Imtiyaz HZ, Simon MC. Hypoxia-inducible factors as essential regulators of inflammation. *Curr Top Microbiol Immunol.* 2010; 345:105–120. [PubMed: 20517715]
45. Gonzalez-Reyes S, et al. Study of TLR3, TLR4 and TLR9 in breast carcinomas and their association with metastasis. *BMC Cancer.* 2010; 10:665. [PubMed: 21129170]
46. Ahmed A, Wang JH, Redmond HP. Silencing of TLR4 Increases Tumor Progression and Lung Metastasis in a Murine Model of Breast Cancer. *Ann Surg Oncol.* 2012 (Epub ahead of print).
47. Etokebe GE, et al. Single-nucleotide polymorphisms in genes encoding toll-like receptor-2-3-4, and-9 in case-control study with breast cancer. *Genet Test Mol Biomarkers.* 2009; 13:729–734. [PubMed: 19810822]
48. Apetoh L, Tesniere A, Ghiringhelli F, Kroemer G, Zitvogel L. Molecular interactions between dying tumor cells and the innate immune system determine the efficacy of conventional anticancer therapies. *Cancer Res.* 2008; 68:4026–4030. [PubMed: 18519658]
49. Sterneck E, et al. Selectively enhanced contextual fear conditioning in mice lacking the transcriptional regulator CCAAT/enhancer binding protein delta. *Proc Natl Acad Sci U S A.* 1998; 95:10908–10913. [PubMed: 9724803]
50. Hoover DL, Nacy CA. Macrophage activation to kill *Leishmania tropica*: defective intracellular killing of amastigotes by macrophages elicited with sterile inflammatory agents. *J Immunol.* 1984; 132:1487–1493. [PubMed: 6363543]
51. van Drogen F, et al. Ubiquitylation of cyclin E requires the sequential function of SCF complexes containing distinct hCdc4 isoforms. *Mol Cell.* 2006; 23:37–48. [PubMed: 16818231]
52. Morrison DK, Heidecker G, Rapp UR, Copeland TD. Identification of the major phosphorylation sites of the Raf-1 kinase. *J Biol Chem.* 1993; 268:17309–17316. [PubMed: 8349614]
53. Roger T, et al. Critical role for Ets, AP-1 and GATA-like transcription factors in regulating mouse Toll-like receptor 4 (Tlr4) gene expression. *Biochem J.* 2005; 387:355–365. [PubMed: 15537384]

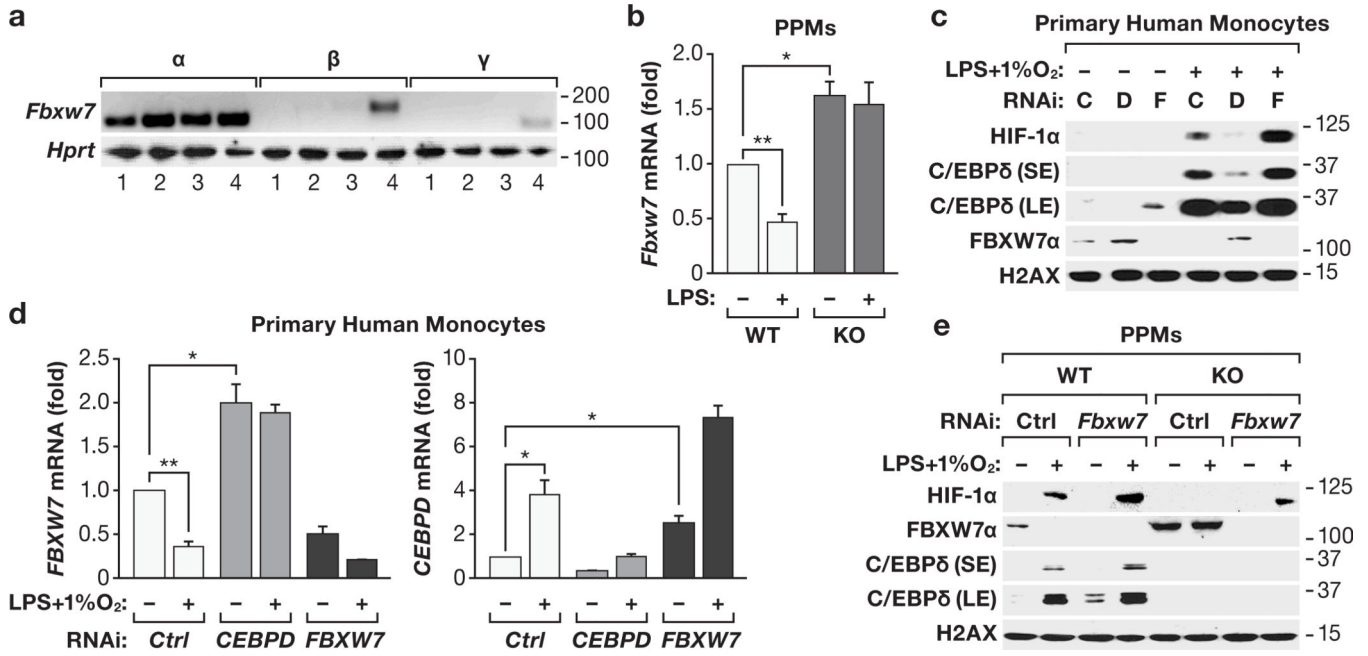


Figure 1. C/EBPδ promotes HIF-1α expression in macrophages through inhibition of FBXW7α
a) RT-PCR analysis of FBXW7 isoform expression from different sources as follows. 1, primary peritoneal macrophages (PPMs); 2, RAW 264.7 cells; 3, MMTV-Neu mammary tumour tissue; 4, primary mouse embryo fibroblasts. Numbers indicate the position of size markers in base pairs. **(b)** RT-qPCR analysis of *Fbxw7* transcript levels in PPMs from WT and *Cebpd*^{-/-} KO mice, cultured +/- LPS (100 ng/ml, 24 h), compared to WT untreated (n=4, **P*<0.05; ***P*<0.001). **(c)** Western analysis of nuclear extract (NE) from primary human monocytes nucleofected with siRNA oligos (C, control; D, *CEBPD*; F, *FBXW7*) and treated with LPS (100 ng/ml) and 1% O₂ (16 h) as indicated. SE, short exposure; LE, long exposure. **(d)** RT-qPCR analysis of *FBXW7* and *CEBPD* transcripts in primary human monocytes as in panel (c) (n=3, **P*<0.05; ***P*<0.001). **(e)** Western analysis of NE from PPMs nucleofected with siRNA oligos and treated with LPS (100 ng/ml) and 1% O₂ for 16 h as indicated. SE, short exposure; LE, long exposure. Where applicable, data are mean±S.E.M., evaluated by two-tailed unequal variance t-test.

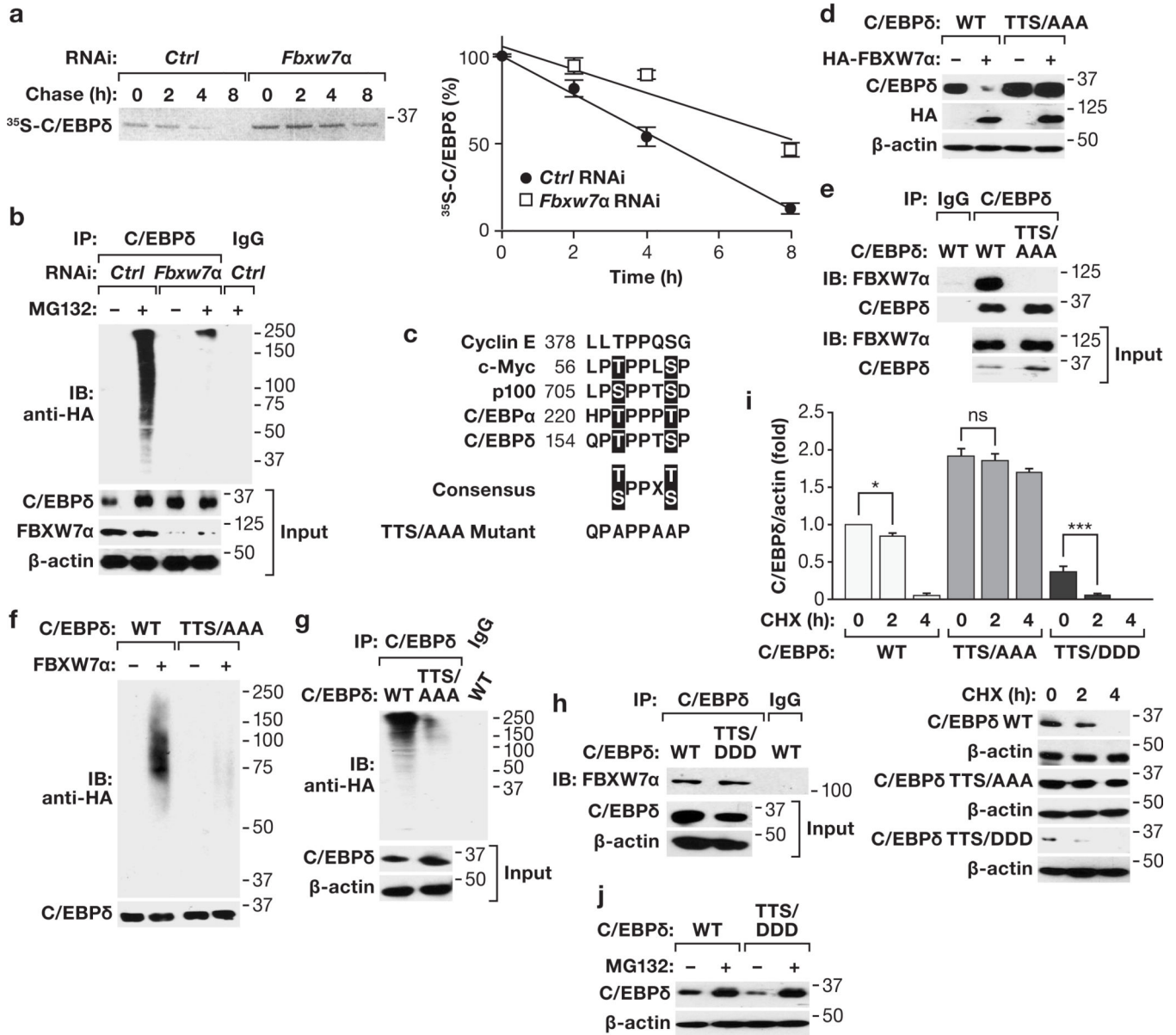


Figure 2. FBXW7α interacts with C/EBPδ and targets it for degradation

(a) RAW 264.7 macrophages were transfected with control or *Fbxw7α* siRNA oligos for 48 h, then pulse-labeled with ³⁵S-methionine/cysteine, followed by chased with excess unlabeled aminoacids for the indicated times. Quantitation of the phosphorimage of C/EBPδ signal is depicted in the graph (mean±S.E.M., n=2–3) and representative primary data are shown. (b) Western analysis of RAW 264.7 cells transfected with HA-ubiquitin expression constructs and control or *Fbxw7α* siRNA oligos and treated ± MG132 (20 μM, 6 h), followed by immunoprecipitation under denatured conditions with anti-C/EBPδ or IgG (with equal aliquots of the indicated extracts). Input (2.5% of lysate) was analyzed as indicated. (c) Alignment of phosphodegron motifs present in known FBXW7 substrates with C/EBPδ and its TTS/AAA mutant. (d) Western analysis of RAW 264.7 cells transfected with WT- or TTS/AAA-C/EBPδ expression plasmids and/or HA-FBXW7α. (e) Western analysis of RAW

264.7 cells transfected with WT or TTS/AAA C/EBP δ expression plasmids and immunoprecipitated with anti-C/EBP δ or IgG and input (2.5% of lysate) as indicated. **(f)** RAW 264.7 cells were transfected with WT- or TTS/AAA-C/EBP δ expression constructs. C/EBP δ was immunoprecipitated and the beads were incubated with FBXW7 α and HA-ubiquitin as indicated (see Methods for details) and analyzed by Western with anti-HA and C/EBP δ antibodies. **(g)** Western analysis of RAW 264.7 cells transfected with WT- or TTS/AAA-C/EBP δ , treated \pm MG132 (20 μ M, 6 h) followed by immunoprecipitation under denatured conditions using anti-C/EBP δ or IgG and input (2.5% of lysate) as indicated. **(h)** Western analysis of RAW 264.7 cells transfected with WT- and TTS/DDD-C/EBP δ for 48 h followed by immunoprecipitation with anti-C/EBP δ or IgG and input (2.5% of lysate) as indicated. **(i)** Western analysis (bottom panel) of RAW 264.7 cells transfected with WT-, TTS/AAA- or TTS/DDD-C/EBP δ expression constructs and treated with CHX as indicated. Quantification (top panel) of the C/EBP δ signal was normalized to actin (n=3, * P <0.05; *** P <0.0001; ns, not significant). **(j)** Western analysis of RAW 264.7 cells transfected with WT- or TTS/DDD-C/EBP δ expression constructs and treated \pm MG132 (20 μ M, 6 h). Where applicable, data are mean \pm S.E.M., evaluated by two-tailed unequal variance t-test.

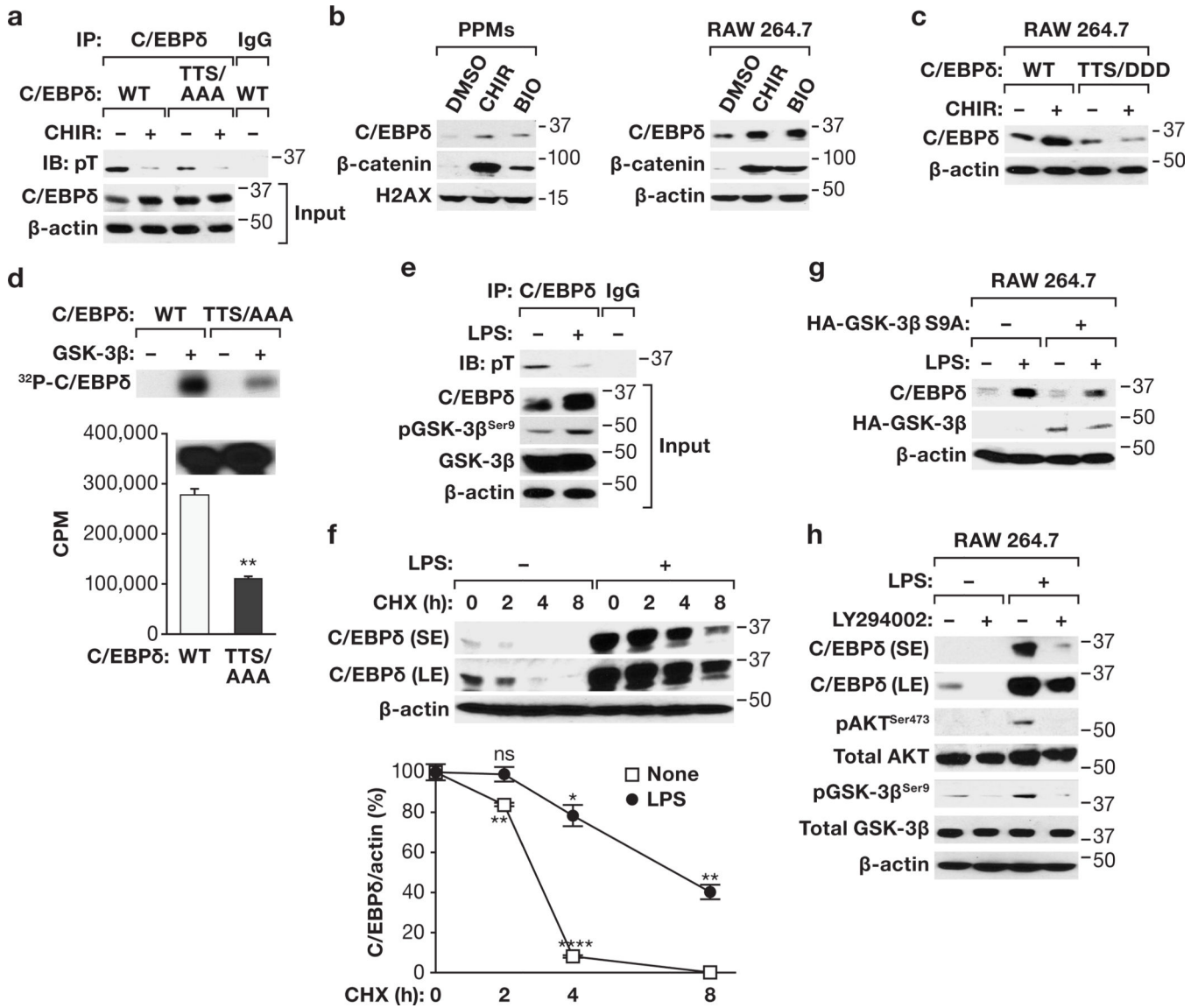


Figure 3. C/EBPδ stability is regulated by GSK-3β phosphorylation

(a) RAW 264.7 cells were transfected with WT or TTS/AAA CEBPδ expression plasmids and treated ± GSK-3β inhibitor CHIR99021 (5 μM, 2 h). Cell extracts were immunoprecipitated with anti-C/EBPδ or IgG (with an aliquot of the indicated extract) and the Western analyzed with anti-phosphothreonine (pT) antibody. (b) Western analysis of NE from PPMs (left panel) or RAW 264.7 cells (right panel) treated with GSK-3β inhibitors CHIR99021 or BIO (6-bromoindirubin-3'-oxime) (5 μM, 2 h). β-catenin, which is known to be targeted for degradation by GSK-3β phosphorylation, served as positive control. (c) Western analysis of RAW 264.7 cells transfected with WT- or TTS/DDD-C/EBPδ expression plasmids and treated ± GSK-3β inhibitor CHIR99021 for 2 h. (d) GSK-3β phosphorylates C/EBPδ *in vitro*. HEK293T cells were transfected with WT- or TTS/AAA-C/EBPδ expression plasmids. C/EBPδ proteins were immunoprecipitated from cell extracts and *in vitro* kinase assay reactions were carried out in the presence or absence of GSK-3β. Samples were resolved by SDS-PAGE and subjected to autoradiography (top panel). Total

radioactivity (bottom panel) incorporated into the C/EBP δ protein was quantified (n=3). Representative input levels of C/EBP δ are shown by Western (inset). (e) RAW 264.7 cells were treated \pm LPS (4 h) and cell extracts were immunoprecipitated with anti-C/EBP δ or IgG antibodies and Western analysis was carried out with anti-phosphothreonine (pT) antibody. Input (2.5% of the lysate) was analyzed as indicated. (f) Western analysis (top panel) of RAW 264.7 cells treated \pm LPS (100 ng/ml, 4 h) followed by CHX for the indicated times, and quantification of C/EBP δ normalized to β -actin signal (bottom graph) compared to respective untreated (n=3, * P <0.05; ** P <0.001; **** P <0.0001). (g) Western analysis of RAW 264.7 cells transfected with HA-GSK-3 β -S9A expression plasmids treated \pm LPS (4 h) as indicated. (h) Western analysis of RAW 264.7 cells pretreated with the PI3K/AKT kinase pathway inhibitor LY294002 (10 μ M, 1 h) followed by LPS (100 ng/ml, 4 h) as indicated. Where applicable, data are mean \pm S.E.M., evaluated by two-tailed unequal variance t-test.

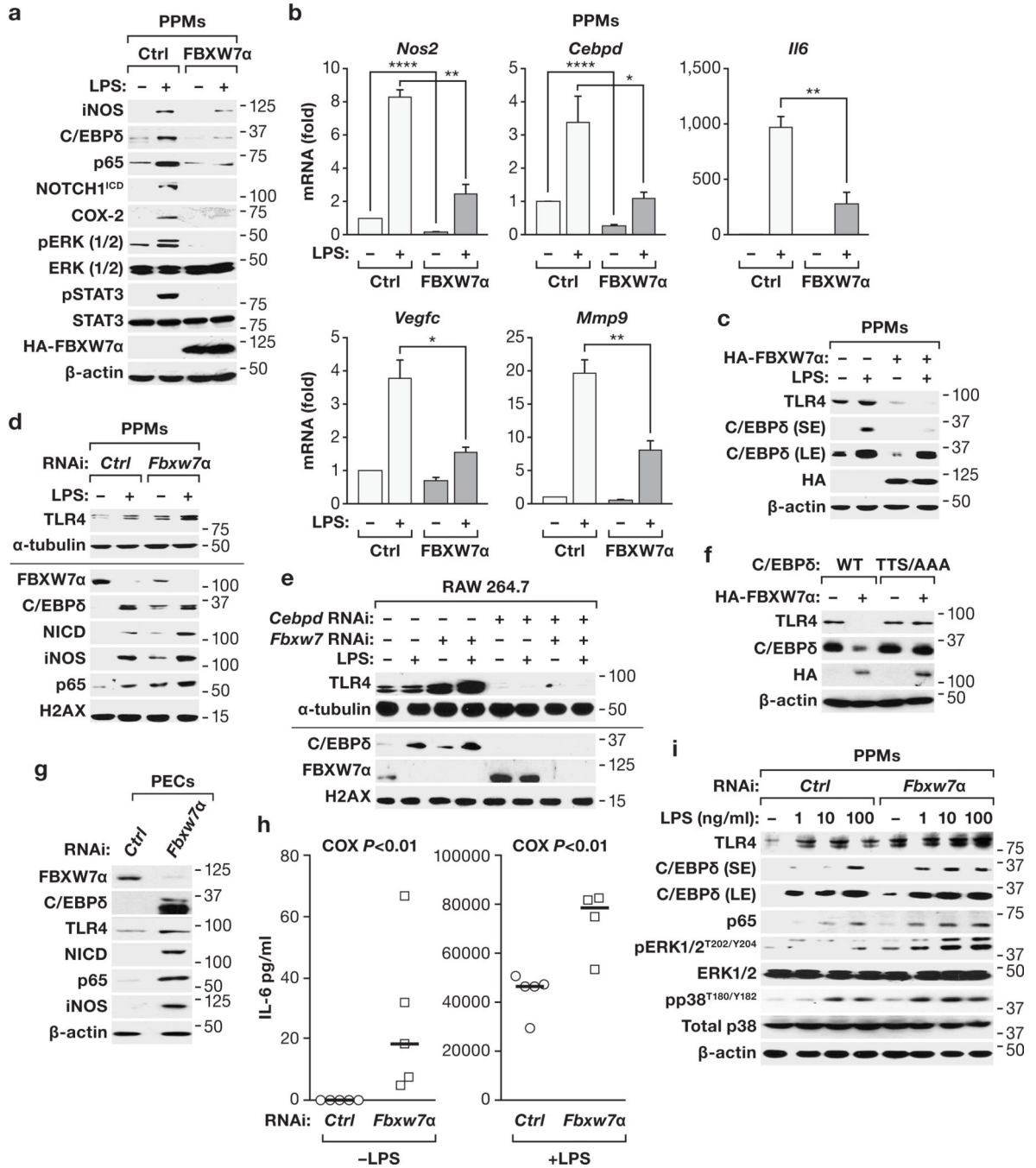


Figure 4. FBXW7 α suppresses TLR4-mediated LPS responses through C/EBP δ
 (a) Western analysis of NE from PPMs transfected with vector or FBXW7 α expression constructs and treated with LPS (100 ng/ml, 16 h) as indicated. (b) RT-qPCR of the indicated mRNA levels in PPMs nucleofected with FBXW7 α expression plasmids and treated with LPS (100 ng/ml, 16 h) as indicated (n=3, * P <0.05, ** P <0.001, **** P <0.0001). (c) Western analysis of PPMs transfected with HA-FBXW7 α and treated with LPS (100 ng/ml, 16h) as indicated. SE, short exposure; LE, long exposure. (d) Western analysis of proteins from PPMs nucleofected with control or *Fbxw7 α* siRNA oligos and

treated \pm LPS (100 ng/ml, 16 h). The line separates analysis of cytoplasmic (top) and nuclear (bottom) extracts. (e) Western analysis of RAW 264.7 macrophages transfected with siRNA oligos against endogenous *Cebpd* or *Fbxw7a* alone or in combination and treated with LPS (100 ng/ml, 16 h) as indicated. The line separates analysis of cytoplasmic (top) and nuclear (bottom) extracts. (f) Western analysis of RAW 264.7 macrophages transfected with the indicated expression plasmids. (g) Western analysis of PECs isolated from FVB/N mice 48 h after injection of RNAi against *Fbxw7a* or control siRNA. (h) Plasma IL-6 concentrations from mice injected with RNAi against *Fbxw7a* or control siRNA for 72 h followed by LPS (40 ng) or vehicle (saline) for 1 h. The horizontal line indicates the median IL-6 concentration (n=4-5, *P* values were determined by the Wilcoxon rank-sum test, *P* < 0.01). (i) Western analysis of PPMs transfected with control or *Fbxw7a* siRNA oligos and treated with LPS (100 ng/ml, 4 h) as indicated. SE, LE; short, long exposure. Where applicable, data are mean \pm S.E.M., evaluated by two-tailed unequal variance t-test (except panel 4h).

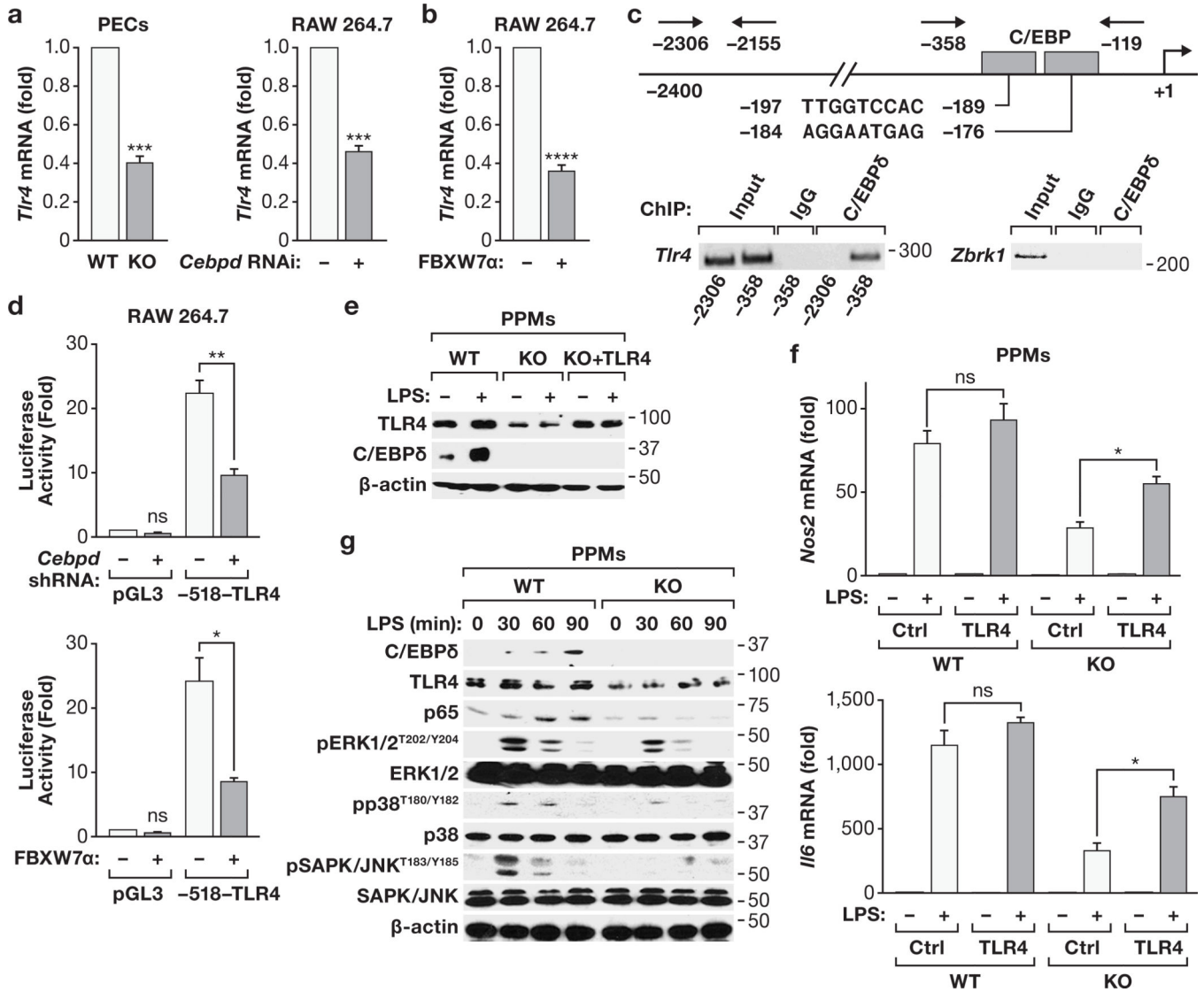


Figure 5. TLR4 is a direct transcriptional target of C/EBPδ
(a) RT-qPCR analysis of *Tlr4* mRNA levels in WT or *Cebpd* KO PECs and in RAW 264.7 macrophages after *Cebpd* silencing (n=3, ****P*<0.001). **(b)** RT-qPCR analysis of *Tlr4* in RAW 264.7 macrophages with or without ectopic FBXW7α (n=3, *****P*<0.0001). **(c)** Schematic of the *Tlr4* promoter with location of putative C/EBP binding sites and of primers used for ChIP. ChIP analysis from PPMs for binding of C/EBPδ to the indicated *Tlr4* promoter regions. IgG and a *Zbrk1* promoter region served as negative controls. Numbers indicate the position of molecular size markers in base pairs. **(d)** Luciferase reporter assay in RAW 264.7 macrophages transfected with the indicated luciferase reporter and shRNA against *Cebpd* (top panel) or FBXW7α expression constructs (bottom panel) (n=3, **P*<0.05, ***P*<0.001). ns, not significant. **(e)** Western analysis of PPMs from WT and *Cebpd* KO mice transfected with TLR4 expression plasmids as indicated. **(f)** RT-qPCR analysis of the indicated mRNA levels in PPMs as in panel (e). (n=3, **P*<0.05; ns, not significant). **(g)** Western analysis of PPMs from WT and *Cebpd* KO mice treated with 200 ng/ml LPS for the

indicated times. Where applicable, data are mean \pm S.E.M., evaluated by two-tailed unequal variance t-test.

Author Manuscript

Author Manuscript

Author Manuscript

Author Manuscript

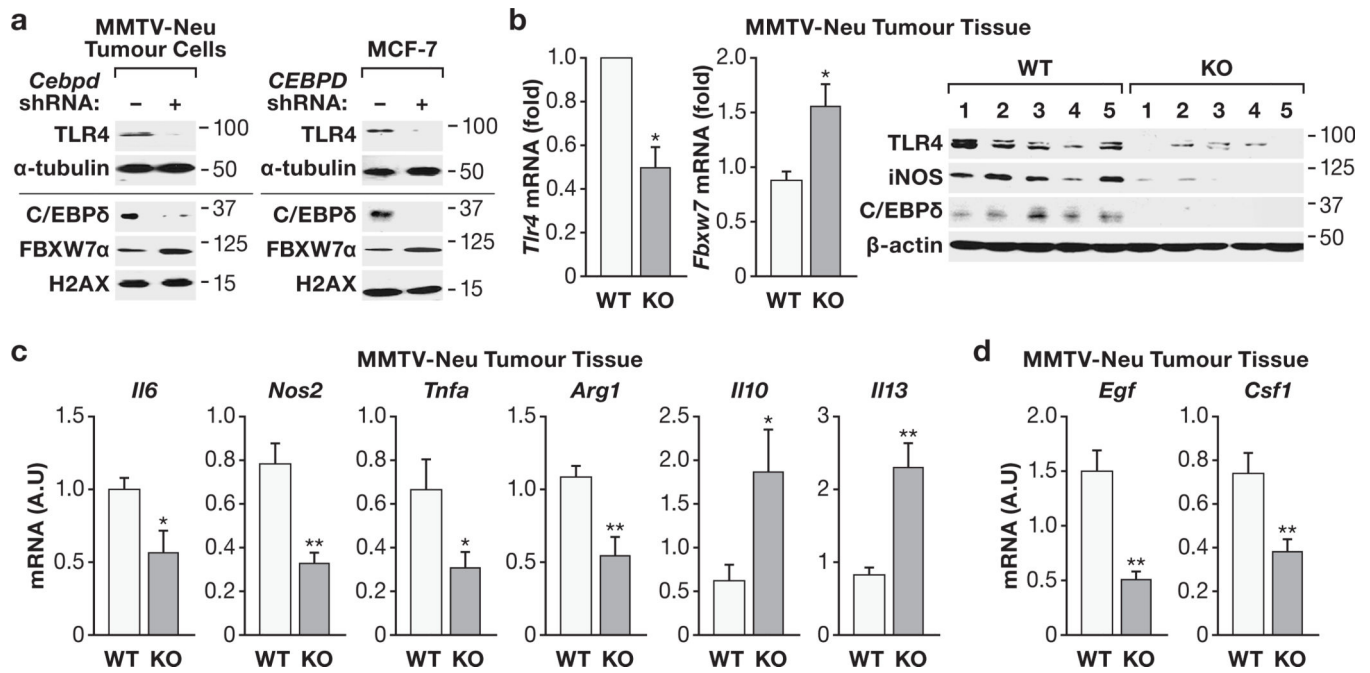


Figure 6. *Cebpd* null tumours exhibit reduced expression of TLR4 and altered expression of inflammatory genes

(a) Western analysis of proteins from an MMTV-Neu tumour cell line or MCF-7 cells with stable shRNA-silencing of C/EBPTM expression or control shRNA. The line separates analysis of cytoplasmic (top) and nuclear (bottom) extracts. (b) RT-qPCR analysis of *Tlr4* and *Fbxw7* mRNA (left panels) and Western analysis (right panel) of protein from MMTV-Neu tumours of WT and *Cebpd* KO mice (n=5, **P*<0.05). (c,d) RT-qPCR analysis of mRNA levels of the indicated genes in MMTV-Neu tumour tissue from WT and *Cebpd* KO mice. A.U., arbitrary units. (n=6, **P*<0.05; ** *P*<0.001). Where applicable, data are mean ±S.E.M., evaluated by two-tailed unequal variance t-test.

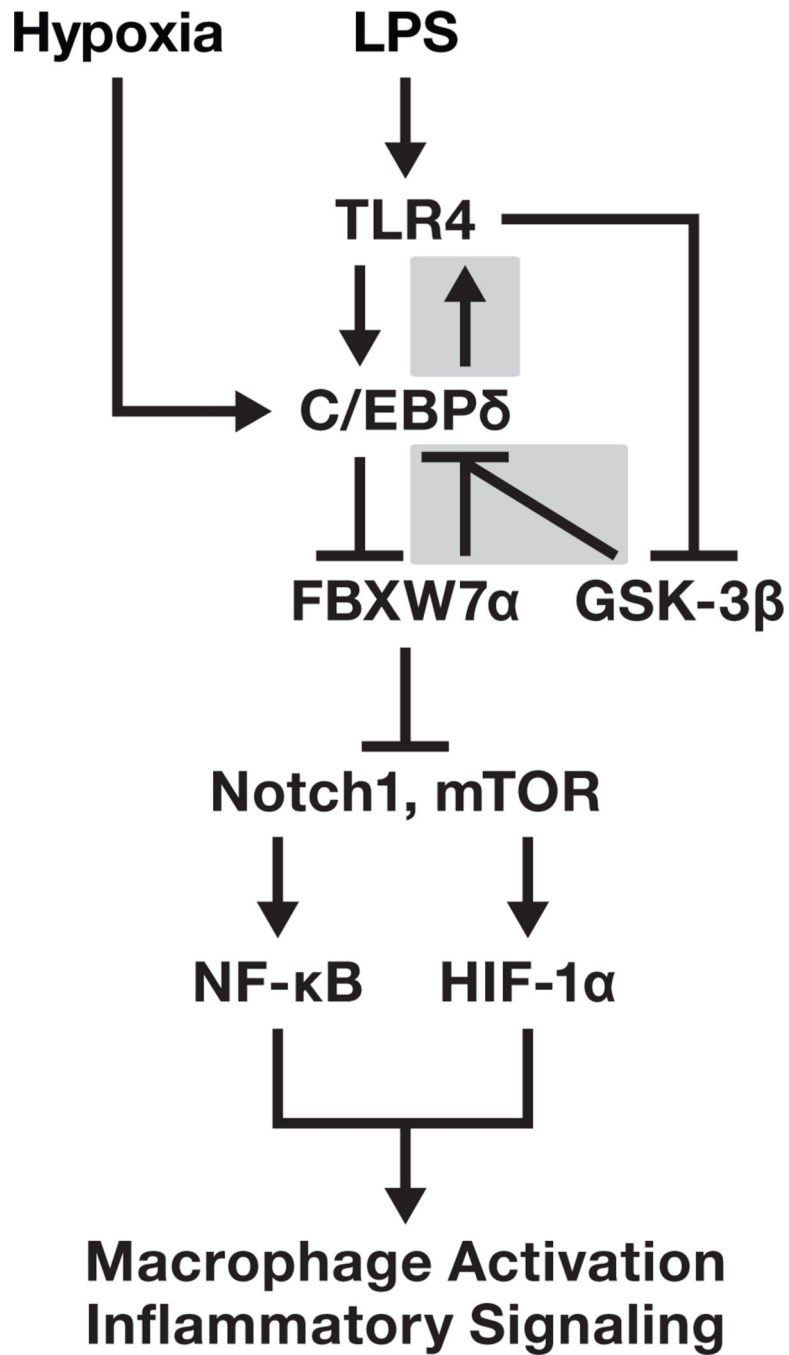


Figure 7. Schematic describing the feedback loops between TLR4, C/EBPδ and FBXW7α that control LPS signaling

The shaded boxes indicate the elements of this pathway that were identified in this study.

Table 1Sites of C/EBP δ phosphorylated by GSK-3 β

Fractions	Edman Degradation	Peptide	Phosphoamino acid
6–7 (P)	4	L.GSTpTPAMY.	T49
68–70 (P)	7 (11)	L.AAAAQPpTPPTSPEPPRGSPGPSL.	T156 (S160)

To identify the phosphorylation sites, labeled WT- and TTS/AAA-C/EBP δ were subjected to in-gel digestion with pepsin (P) followed by HPLC analysis. Edman degradation and phosphoamino acid analysis was performed on the indicated fractions.

Author Manuscript

Author Manuscript

Author Manuscript

Author Manuscript